Journal of the European Ceramic Society **19** (1999) 2685–2694

PII: S0955-2219(99)00048-5
0955-2219/99/$ - see front matter

Nitrogen-containing Apatite

Stefan Habelitz,[a] Luis Pascual,[b]* and Alicia Durán[b]

[a]Universität Erlangen-Nürnberg, Wekstoffwissenschaften III, Martensstr. 5, 91058 Erlangen, Germany
[b]Instituto de Cerámica y Vidrio (CSIC), Ctra. de Valencia, km 24, 300, 28500 Arganda del Rey, Spain

(Received 1 September 1998; accepted 30 January 1999)

Abstract

Two commercial hydroxyapatites were treated in dry ammonia at temperatures between 800 and 1300°C for different times up to 30 h. Nitrogen was incorporated with a maximum content of 3·7 wt% in presence of graphite. X-ray diffraction studies show no important phase transformation by the incorporation of nitrogen up to 1200°C. Treatments at temperatures above 1200°C resulted in the formation of CaO or $Ca(OH)_2$. ^{31}P NMR studies indicate no direct bonding of nitrogen and phosphorous. Infrared spectra show increasing intensities of four new bands at 3250, 2016, 1966 and 700 cm^{-1} with increasing nitrogen contents, while the OH-bands at 3570 and 630 cm^{-1} vanish. Taking into account results of the carbon content, XRD, NMR and IR spectra it is suggested that nitrogen enters into the structure as $[CN_2]^{2-}$ ion, substituting $[OH]^-$ groups, and forming cyanamidapatite $Ca_{10}(PO_4)_6(CN_2)$.

Keywords: nitridation, spectroscopy, apatite.

1 Introduction

Calcium hydroxyapatite has received considerable attention for a number of years as an important inorganic constituent of human bones and teeth.[1] Further, it is known that these compounds present a high adsorption power and catalytic activity, and that they perform a series of cationic and anionic exchange reactions.[2]

Hydroxyapatite $Ca_{10}(PO_4)_6(OH)_2$, (HA) is a member of the apatite family of minerals which have the general formula $A_{10}(BO_4)_6X_2$. The structure of hydroxyapatites is essentially constituted by the ionic crystals built up from A^{2+}, BO_4^{3-} and X^- ions.[3,4] The arrangement of the BO_4^{3-} tetrahedra approximates to a closed-packed hexagonal lattice, in which the A^{2+} and X^- ions are located in the tetrahedric sites. Hence, apatites belong to space-group $P6_3/m$ or $P2_1/b$. Most of A^{2+} ions form equilateral triangles, which are separated by two larger triangles formed by the O^{2-} ions of three different phosphate tetrahedra. The plane of these triangles are parallel to each other and the distance between planes is about 6·5 Å. This parallel arrangement of the triangle planes composes channels along the centres of the triangles perpendicular to the hexagonal axis. The gravity centres of the triangles are in a staggered configuration and the X^- ions are contained into the channels formed by A^{2+} ions. In the pseudo-hexagonal unit cell of hydroxyapatite, hydroxyl ions are located in the center of triangles of Ca^{2+} ions and oriented with the hydrogen atom pointing the direction of the *c*-axis.[5]

The atomic arrangement of HA admits large deviations from its theoretical composition, and nonstoichiometric forms and ionic substitutions of the Ca^{2+}, PO_4^{3-} groups are common.[6–8] The Ca^{2+} cations can be substituted by Na^+, K^+, Mg^{2+}, Sr^{2+}, Pb^{2+} or Mn^{2+} and the PO_4^{3-} anions by AsO_4^{3-}, SO_4^{2-} or CO_3^{2-} up to a certain amount without destroying the apatitic structure.[9–13]

An exchange of the OH^- ions for others of similar size is also very frequent. The exchange ability of the OH^- groups derives from their location in the apatite lattice. Several papers describe good mobility for diffusion of hydroxyl groups along this channels at high temperature.[2,6–10] At temperatures above 900°C hydroxyapatite interchanges OH^- groups by Cl^-, O^{2-} and CO_3^{2-} ions in a gas flow of each of these molecules, a property which is used for the preparation of chlor-, oxy- and carbonated apatite.[5,13–16] OH^- ions can be also exchanged by F^- ions at room temperature, what contributes to caries inhibition of human dental enamel.

*To whom correspondence should be addressed. Fax: +349-91-870-0550; e-mail: lpascual@icv.csic.es

The aim of this work has been to prepare a nitrogen-containing apatite by treatment of commercial hydroxyapatite in a dry ammonia atmosphere at high temperatures. This type of procedure has been applied in phosphate glasses, to modify different properties, specially chemical and thermal ones.[17,18] The nitrogen-containing groups will be characterized as well as those that are replaced in the hydroxyapatite network during the nitridation process. The nitridation kinetics and the structural changes in the hydroxyapatite network provoked by nitrogen incorporation will be also studied.

2 Experimental

2.1 Starting materials

Two commercial hydroxyapatites were used as starting materials for nitridation: (a) a fine semi-amorphous calcium defect hydroxyapatite by Fluka, Buchs (CH), named CDHA, and (b) a well crystallized hydroxyapatite with a Ca/P stoichiometric ratio by Betthys, Bettlach (CH), named Ceros 80, frequently used in medicine for filling bone defects.

2.2 Thermal treatments

Approximately 1 g of each type of hydroxyapatite were subjected to different thermal treatments in a dry flowing ammonia atmosphere. The samples were placed in an airtight furnace and nitrogen was flowed through to eliminate the air at the same time that temperature was raised up. When temperature was about 600°C the nitrogen flow was replaced by ammonia ($500\,cm^3\ min^{-1}$) and the furnace temperature was raised up to the treatment selected temperature between 800 and 1300°C. The temperature and the ammonia flow were kept constant until the end of treatment, from 1 to 16 h. Finally, the furnace was cooled down under ammonia atmosphere. Alumina and graphite crucibles were used as containers and in some cases graphite powder was put aside the graphite and alumina crucibles containing the sample.

Thermal treatments in Ar atmosphere were performed under the same conditions of those in ammonia in order to separate thermal effects from nitridation effects on hydroxyapatite samples.

2.3 Characterization

Chemical analysis of calcium, phosphorus, sodium and magnesium were made by inductive coupled plasma, ICP, with a Jobin-Yvon sequential spectrometer, model JY-38 VHR. The specific surface area was measured by the Brunauer–Emmet–Teller method, BET, with an Quantachrome, model Monosorb. Nitrogen analysis were performed by inert gas fusion method using a Leco type differential oxygen and nitrogen analyser, TC-436 model. Carbon analysis were made by the infrared absorption method at 85 Hz with a carbon and sulphur Leco analyser C-200 model. All the samples were treated at 500°C for half an hour before the analysis to eliminate the CO_2 adsorbed on the surface.

X-ray diffraction powder patterns (DRX), were obtained on a Siemens diffractometer with CuK_α radiation at 45 kV, 35 mA, operating in the step scanning mode. The step size was 0·025 (2Θ) and the counting time per step was 3 s in a 2Θ range from 25 to 67°. For the calculation of the unit cell constants by least-square fit only defined diffraction peaks with $2\Theta > 45°$ were selected.

^{31}P magic angle spinning nuclear magnetic resonance, (^{31}P-MASS-NMR), spectra were acquired on a Bruker MSL-400 spectrometer operating at 161·977 Mhz. Magic angle sample spinning was carried out with about 0·1 g samples, using spinning speeds of 4 khz. Chemical shifts were measured with respect to an external reference of 85% H_3PO_4 with an estimated deviation of 0·5 ppm.

Infrared spectra from 4000 to $400\,cm^{-1}$ were recorded on a Fourier transform infrared spectrophotometer (FTIR) Perkin–Elmer model 1760-X on disks of 300 mg KBr adding 1·5 mg of Ceros 80 or 0·5 mg of CDHA, respectively. To eliminate adsorbed water disks were dried at 100°C and cooled down to room temperature in dry air before measurements.

3 Results

3.1 Characterization of starting materials

CDHA hydroxyapatite shows a high specific surface area of $62\,m^2\ g^{-1}$ and a Ca/P ratio of 1·52. This Ca/P ratio is notably lower than the stoichiometric value of 1·67. The carbon content of this hydroxyapatite, measured as CO_2, is 0·15 wt%.

Ceros 80 hydroxyapatite with a Ca/P stoichiometric ratio consists of agglomerates with two grain size distributions between 0·7 and 1·4 mm, and 1·4 and 2·8 mm, and constitutes a system of closed macro- and micro pores occuping about 60% of the total volume. Its measured specific surface area is as low as $0{\cdot}07\,m^2\ g^{-1}$, and the carbon content is 0·05 wt%.

The X-ray diffraction spectra of both hydroxyapatites used as starting products are showed in Fig. 1. It is observed a great difference between the crystallization grade of both materials that reveals the semiamorphous character of hydroxyapatite CDHA. Only peaks corresponding to hydroxyapatite phase can be detected in both diffraction patterns.

3.2 Nitridation kinetics

The kinetics of nitrogen incorporation into hydroxyapatite was studied by measurements of the nitrogen content as a function of the temperature and time of the thermal treatment. For the studied temperature and time ranges nitrogen incorporation can be only detected when using graphite crucibles or when graphite powder was placed side by side to the alumina crucibles. When alumina crucibles were used in absence of graphite, no or insignificant amounts of nitrogen could be incorporated.

The nitridation kinetics was studied as a function of temperature for a constant time of 7 h, in the range of 800 to 1300°C. Figure 2 shows the nitrogen content of CDHA and Ceros 80 hydroxyapatites as a function of the treatment temperature in ammonia atmosphere. The nitrogen content incorporated into hydroxyapatite CDHA, treated during 7 h at different temperatures, is about 1 wt% at treatment temperatures below 900°C and increases sharply between 900 and 950°C up to about 2·7 wt%. Heat treatments above 1000°C cause a slower increase of nitrogen content, which reaches a maximun of 3·7 wt% for temperatures about 1200°C. Treatments at higher temperatures resulted in lower amounts of nitrogen.

Hydroxyapatite Ceros 80 do not incorporate any noticeable quantity of nitrogen at temperatures below 1050°C. From this temperature, the nitrogen content incorporated into the samples increases with raising temperatures up to a maximum value of 2·1 wt% of N_2 at 1200°C for 7 h.

The kinetics as a function of treatment time was studied at a constant temperature of 1200°C, corresponding to the highest nitrogen values incorporated for a thermal treatment time of 7 h. Figure 3 shows the dependence of the nitrogen content with the duration of ammonia treatments at 1200°C. Nitrogen content incorporated into CDHA increases very sharply reaching values from 3 to 3·5 wt% for times from 1 to 7 h, while Ceros 80 nitrogen concentration reaches a maximun value of 1·5–2·1 wt% in 7 h of thermal treatment. Thermal treatments at 1200°C for times longer that 7 h yielded in both hydroxyapatites a sharp drop of the nitrogen content and elementary phosphorus could be observed on the wall furnace.

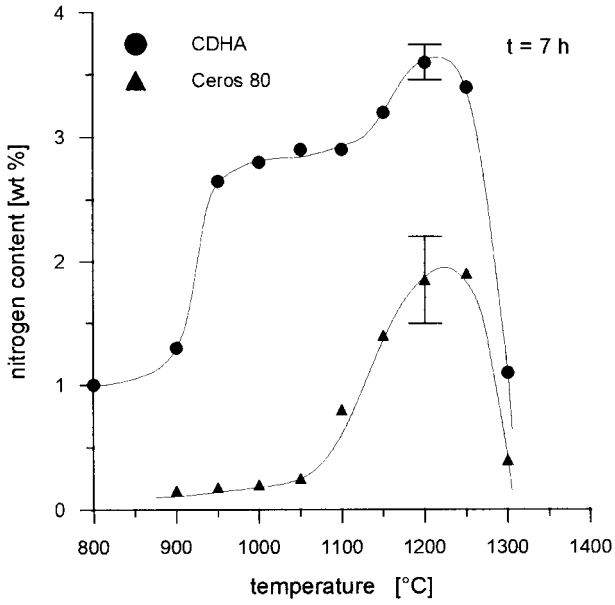

Fig. 2. Nitrogen content of CDHA and Ceros 80 hydroxyapatites after ammonia treatment of 7 h as a function of temperature.

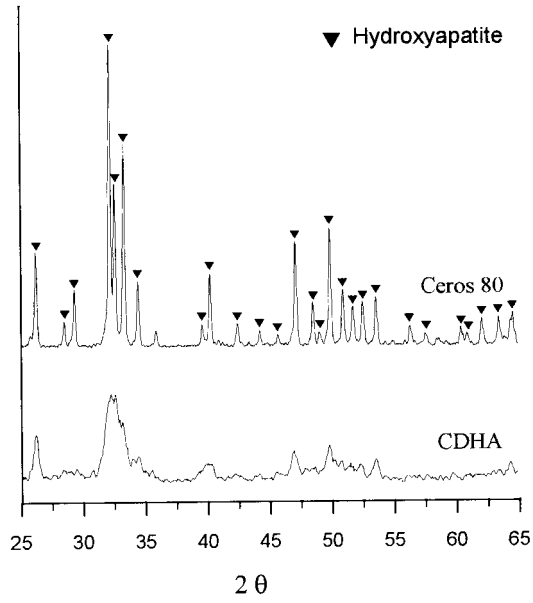

Fig. 1. XRD diffraction spectra of the hydroxyapatites used as starting materials.

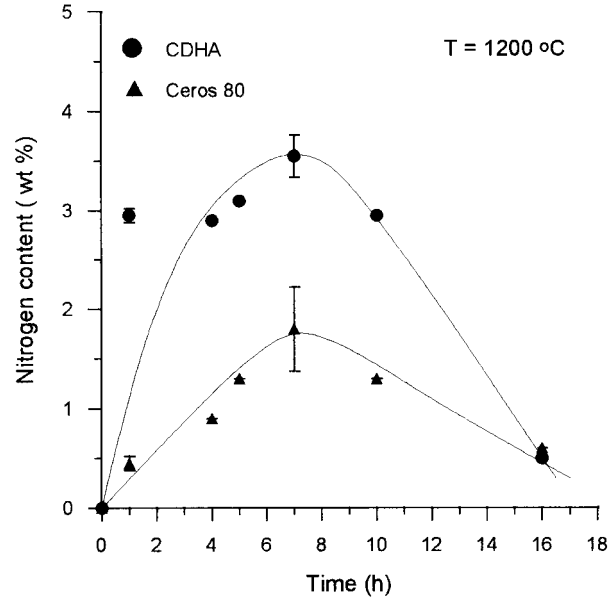

Fig. 3. Nitrogen content of CDHA and Ceros 80 hydroxyapatites as a function of time of thermal treatment at a fixed temperature of 1200°C.

3.3 XRD analysis

Figures 4 and 5 show the XRD patterns of samples before and after ammonia treatments in the 2Θ-range of 25 to 67°.

Untreated samples of CDHA show diffuse patterns indicating a semi-amorphous structure, with small diameters of the crystals (Fig. 4).The increase of the nitrogen content from 1 to 3·7 wt% causes a progressive sharpening of the X-ray patterns as the crystallinity of samples increases. The XRD patterns of CDHA treated at temperatures below 1200°C do not change significantly by the introduction of nitrogen, the prevailing phase being hydroxyapatite. Only small peaks at 2Θ = 30·3 and 30·9 indicate the formation of α and β-tricalcium phosphate, α-TCP and β-TCP, respectively, which proportions have been evaluated to be less than 5 wt%.

Treatments of CDHA hydroxyapatite at temperatures above 1200°C lead to destruction of the hydroxyapatite network. XRD patterns of CDHA treated for 7 h at 1300°C in dry ammonia, and containing a 1 wt% N_2, show that calcium hydroxide and graphite are the crystalline phases only present. The graphite content of these samples could arise from the crucible contamination during the thermal treatment.

The XRD pattern of untreated Ceros 80 corresponds to a high crystalline apatite. After ammonia treatments up to 1200°C, with nitrogen incorporation up to 2·1 wt%, patterns do not change significantly and the apatite phase is stable and dominant (Fig. 5). Only the peak at 2Θ = 38°, indicating CaO, differs from the original hydroxyapatite spectrum. As in CDHA, treatments at 1200°C for 16 h result in a total phase transformation of Ceros 80. XRD patterns of $Ca(OH)_2$ appear and no peak corresponding to apatitic phase can be identified.

The calculated lattice parameters of the starting materials and the nitrogen containing apatites are presented in Table 1. In comparison

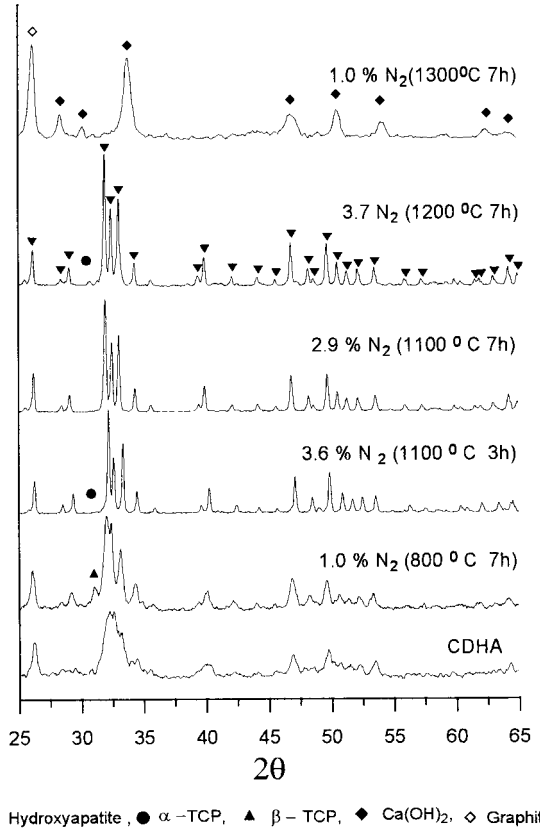

Fig. 4. XRD patterns of CDHA hydroxyapatite before and after different thermal treatments in ammonia atmosphere.

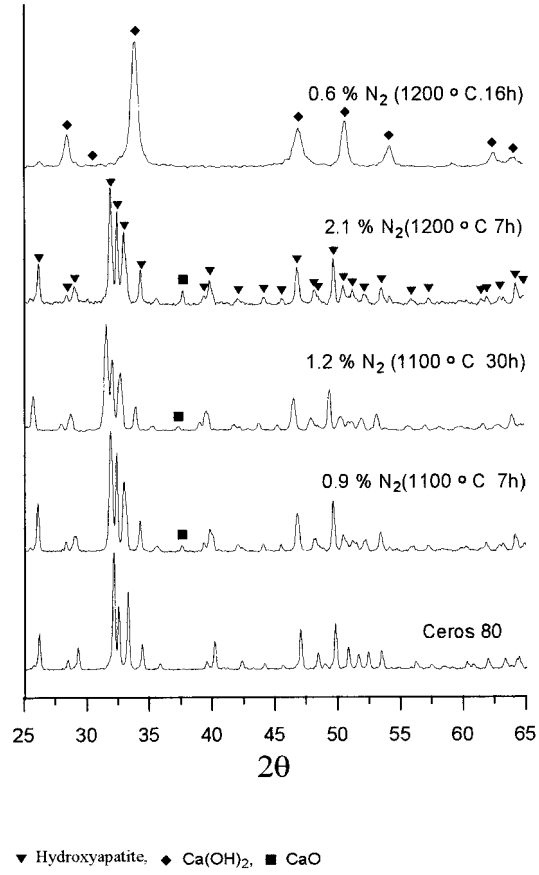

Fig. 5. XRD patterns of Ceros 80 hydroxyapatite as received and after different thermal treatments in ammonia atmosphere.

Table 1. Lattice parameters of CDHA and Ceros 80 nitrogen containing apatites

Sample	*Parameter* a *(Å)*	*Parameter* c *(Å)*	*Standard deviation*
Ceros 80, as received	9·383	6·862	0·991
Ceros 80 0·9 wt% N_2 (1100°C, 7 h)	9·420	6·849	0·995
Ceros 80 2·1 wt% N_2 (1200°C, 7 h)	9·419	6·842	0·994
CDHA 2·9 wt% N_2 (1100°C, 7 h)	9·421	6·844	1·002
CDHA 3·7 wt% N_2 (1200°C, 7 h)	9·424	6·852	0·983

with hydroxyapatite from JCPDS No. 9-432, a small decrease of 0·02 Å is observed for the *c*-axis while the *a*-parameter increases (0·04 Å) by nitrogen incorporation.

X-ray pattern of Ceros 80 hydroxyapatite treated up to 1200°C in an argon atmosphere shows the characteristic peak of the apatite phase indicating that no changes other than dehydroxilation have occurred. On the contrary, XRD pattern of the amorphous CDHA hydroxyapatite shows the formation of α-$Ca_3(PO_4)_2$.

3.4 ^{31}P-MASS-NMR studies

Figure 6 shows the ^{31}P-MASS-NMR spectra of CDHA before and after ammonia treatment. The spectrum of the untreated sample shows a single peak at 2·8056 ppm characteristic of monophase apatite.[19] In the spectrum of a sample treated at 1100°C for 7 h and containing 2·8 wt% of nitrogen, only the single peak could be detected, indicating no changes in the phosphorus bonding state by nitrogen incorporation. The spectrum shows a sharpening of the peak after heat treatment, which is attributed to higher crystallinity.

Figure 7 shows the ^{31}P-MASS-NMR spectrum of untreated Ceros 80 compared to the spectrum of Ceros 80 with 1·5 wt% of nitrogen treated at 1200°C for 7 h. The characteristic single peak corresponding to $[PO_4]^{3-}$ isolated tetrahedra of apatites remains after ammonia treatment and nitrogen incorporation.

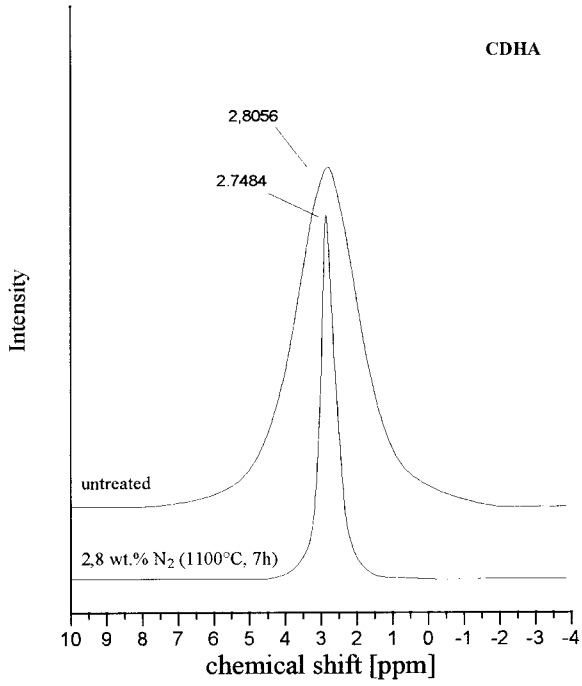

Fig. 6. ^{31}P NMR spectra of untreated CDHA hydroxyapatite and after treatment at 1100°C for 7 h.

3.5 FTIR studies

Figures 8(a)–(d) and 9(a)–(e) show the infrared spectra of hydroxyapatites CDHA and Ceros 80 before and after different thermal treatments in ammonia atmosphere. The infrared spectra of

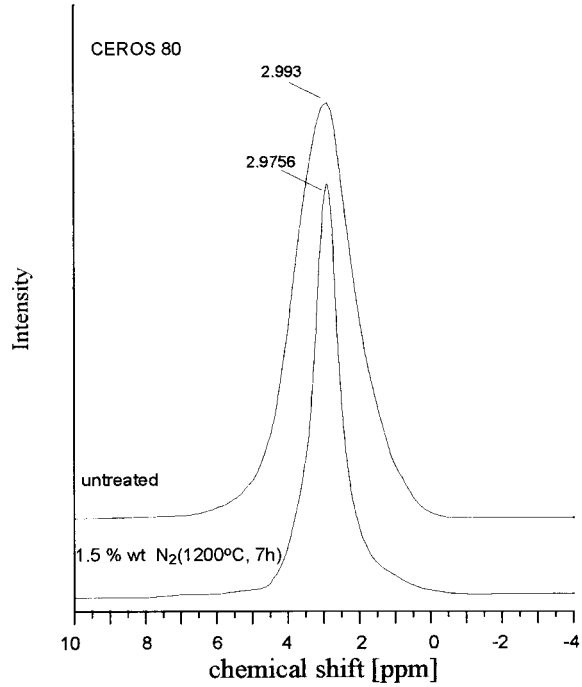

Fig. 7. ^{31}P NMR spectra of untreated Ceros 80 hydroxyapatite and after treatment at 1200°C for 7 h.

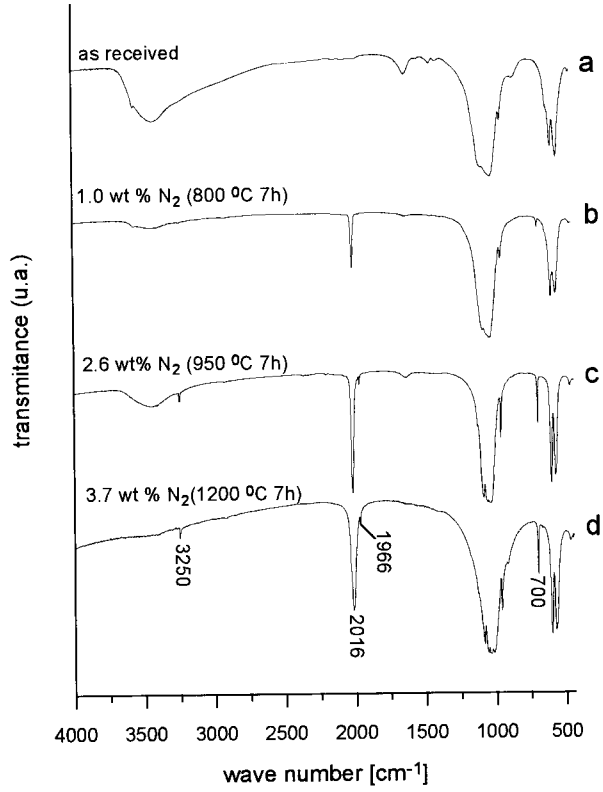

Fig. 8. (a)-(d) IR absorption spectra of CDHA hydroxyapatites, as received and treated at different temperatures and times in ammonia atmosphere.

CDHA and Ceros 80 [Figs 8(a) and 9(a)] show bands corresponding to the characteristic vibrational modes of tetraedral $[PO_4]^{3-}$, $[CO_3]^{2-}$ and $[OH]^-$ groups.[20–22]

Theoretically, there are four vibrational modes for phosphate ions, ν_1, ν_2, ν_3 and ν_4 that are Raman and infrared active.[21,22] Bands in the region of 1190 to 976 cm^{-1} are due to ν_3 vibrational mode of phosphate group. Phosphate ν_1 band is present at near 960 cm^{-1} and can be observed in all spectra of hydroxyapatite and carbonated apatites. Phosphate ν_4 band is present in the region of 600 and 560 cm^{-1}. Two sites appear in the case of carbonated apatites, centered at 603 and 567 cm^{-1}, and three sites are observed in hydroxyapatites at 633, 603 and 565 cm^{-1}. Phosphate vibration ν_2 is normally observed as weak bands in the 475 and 440 cm^{-1} region. In Ceros 80 and CDHA hydroxyapatites infrared spectra, only one peak appears at 472 cm^{-1}.

The OH vibrations at 3570 and 630 cm^{-1} are well defined in Ceros 80. In CDHA these bands are partly overlapped by adsorbed water bands and not so well pronounced because of the low crystallinity of this material.

Bands at 1450, 1425 and 879 cm^{-1} in CDHA are attributed to a substitution of phosphate by carbonate ions[13,23,24] although band at 876 cm^{-1} has also been assigned to O–H bond of HPO_4 group.

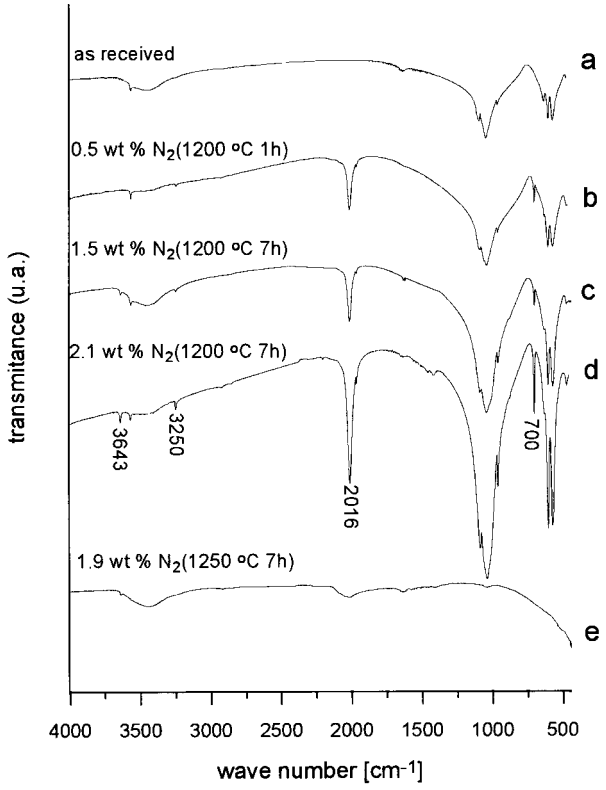

Fig. 9. (a)–(e) IR absorption spectra of Ceros 80 hydroxyapatites, as received and treated at different temperatures and times in ammonia atmosphere.

After ammonia treatment and incorporation of nitrogen several new bands appear. Bands at 1120, 1010, 982 and 951 cm^{-1} in CDHA [Fig. 8(c)] can be assigned to β-TCP.[24] The band at 3643 cm^{-1} indicates the formation of $Ca(OH)_2$ in Ceros 80 [Fig. 9(b)–(d)].[25] However, the bands at 3250, 2016, 1966 and 700 cm^{-1} cannot be attributed to any calcium phosphate formed by phase transformation during heat treatments. These bands only appear in samples containing nitrogen. The bands at 2016 and 700 cm^{-1} are very sharp and intensive and even appear for nitrogen contents as low as 0·5 wt% [Fig. 9(b)]. The 3250 and 1966 cm^{-1} bands are weaker and can only be detected at nitrogen contents higher than 0·5 wt%. The intensities of these four bands increase with the amount of nitrogen, maintaining a constant ratio among them. On the other hand, the OH- bands decrease and finally disappear for a nitrogen content of 2·6 wt% [Fig. 8(c)].

3.6 Carbon analysis

The carbon content of particular samples was also analysed and the results are represented in Table 2 in relation to nitrogen content.

4 Discussion

The studies of the behaviour of two commercial hydroxyapatites in dry ammonia at high temperature have shown that both hydroxyapatites incorporate nitrogen. Nitrogen incorporation was only observed when graphite crucibles were used for the ammonia treatments or in presence of graphite when alumina crucibles were used. This fact suggests that graphite participates in the nitridation reaction by producing a highly reducing atmosphere, acting as a catalyst for the nitridation reaction or incorporating into the apatitic phase as a kind of nitrogen compound. Hydroxyapatite is a special case of material with an open structure that contains ions with a very high mobility as part of the crystalline network. It could accommodate some quantities of nitrogenous molecules if the are thermally stable in ammonia atmosphere. The kinetics studies have shown that the amount of nitrogen introduced increases with time and temperature, reaches a maximum after treatments at

Table 2. Carbon content of CDHA nitrided apatite

Sample	*Carbon content wt%*	*C/N relation*
CDHA as received	0·15	—
CDHA 2·8 wt% N_2	1·31	0·46
CDHA 3·2 wt% N_2	1·27	0·40

1200°C for 7 h and finally decreases for treatments at higher temperature and/or for longer times.

It is shown from literature[26] that stoichiometric hydroxyapatite dehydrates during heating at temperatures between 900 and 1200°C due to the reaction:

$$Ca_{10}(PO_4)_6(OH)_2 \rightarrow Ca_{10}(PO_4)_6O + H_2O \quad (1)$$

One mole of water is lost for each mole of hydroxyapatite to turn into oxyapatite. The XRD pattern of oxyapatite is very similar to that of hydroxyapatite. The loss of water, however, can be observed by the decrease in the IR bands intensity assigned to OH vibrations at 3570 and 630 cm^{-1}.[26]

Further heating at temperatures above 1450°C causes thermal decomposition of the oxyapatite into tricalciumphosphate, α-$Ca_3(PO_4)_2$, and tetracalciumphosphate, $Ca_4P_2O_9$.[23]

$$Ca_{10}(PO_4)_6O \rightarrow 2Ca_3(PO_4)_2 + Ca_4P_2O_9 \quad (2)$$

Calcium deficient hydroxyapatites decompose at lower temperatures to stoichiometric hydroxyapatite and tricalcium phosphate, TCP, according to its degree of deficiency[27]

$$Ca_{10-x}(PO_4)_{6-x}(HPO_4)_x(HO)_{2-x} \rightarrow (1-x)Ca_{10}(PO_4)_6(OH)_2 + 3xCa_3(PO_4)_2 + xH_2O \quad (3)$$

In the present study, heat treatments of calcium deficient hydroxyapatite, CDHA, in air or in argon atmospheres resulted in a decomposition at temperatures above 900°C due to reaction 3. However, in dry ammonia CDHA was stable up to temperatures of 1200°C. Thus, the ammonia atmosphere stabilizes the apatitic structure, confirming the role of nitrogen and excluding the possibility that changes are only produced by thermal effect.

After ammonia treatments and introduction of nitrogen up to the maximum contents, the XRD patterns of both stoichiometric and calcium deficient hydroxyapatites correspond to calcium phosphate apatite of space group $P2_1/b$ (JCPDS-file 9-432). No other peaks have been found, which could indicate a change of symmetry as in the chlor-[13] or carbonated apatite.[5] Neither other peak has been detected indicating the presence of any known crystalline nitrogen-containing phase. The formation of a nitrogen-containing glassy phase can be excluded, since the crystallinity of semi-amorphous hydroxyapatite CDHA increases with nitrogen incorporation. The XRD patterns (Figs 4 and 5) show that after treatments at temperatures of 1300°C for 7 h or at 1200°C for 16 h, $Ca(OH)_2$ and graphite are present. That is a consequence of the thermal decomposition of hydroxyapatite with phosphate reduction to elemental red phosphorus, P_4, provoking the destruction of the crystalline network.

Calculation of the lattice parameter shows that the introduction of nitrogen has not any significant effect on the unit cell dimensions. The comparison with hydroxyapatite lattice parameters from JCPDS-file-9-432 ($a = 9{\cdot}41800$ Å, $c = 6{\cdot}88400$ Å) shows a small shortening of the c-axis while the a-axis becomes longer by about 0·04 Å. This change may be compared with that produced by other substitutions. For example, Cl^- interchange for OH^- ions causes a change from $a = 9{\cdot}4214$ Å, $c = 6{\cdot}8814$ Å to $a = 9{\cdot}628$ Å, $c = 6{\cdot}764$ Å[5,11] and Sr^{2+} substitution for Ca^{2+} causes a lengthening of the a- and c-axes to $a = 9{\cdot}76$ Å, $c = 7{\cdot}27$ Å.[11] The changes in the lattice parameters must be indicative of the type of substitution occurring. More important changes occur when a network ion is replaced and it frequently provokes changes in IR spectra. An interesting example is that of the hydroxyl or phosphate substitution by carbonate.[5] When the phosphate tetrahedron is replaced by carbonate a shortening of the a parameter occurs from 9·42 to 9·30 Å for 22 wt% of carbonate content. At the same time the IR band of the PO_4^{3-} group at 630 cm^{-1} becomes wider and the intensity of that at 1050 cm^{-1} decreases and even disappears. Only a little change in network parameters will be expected when the ions replaced are these located along the channels of the hydroxyapatite network. If hydroxyapatite is treated at high temperature in a dry CO_2 atmosphere hydroxyl groups are replaced by carbonate ions. This event causes a lengthening of the a parameter from 9·42 to 9·58 Å for a carbonate content of 6 wt% and the IR spectra are similar to those of natural hydroxyapatites francolite and dahllite.[5]

The small changes observed in hydroxyapatite network parameters by nitrogen incorporation would indicate that the introduced ions do not disturb strongly the apatitic lattice and thus the exchanged ions should be of similar size, charge and electronegativity.[27] Likewise, these facts suggest that the OH^- ions, more than the phosphate groups, are substituted during the thermal treatments.

^{31}P NMR spectra of both hydroxyapatites before and after ammonia treatment confirm that no changes in phosphate groups structure result as a consequence of ammonia treatment. High-resolution ^{31}P NMR of solid calcium phosphates, including stoichiometric and nonstoichiometric hydroxyapatites, exhibit a single signal belonging to isolated phosphate groups.[19,28,29] This single signal is clearly different from those of tricalcium, tetracalcium and the other hydrated and protonated phosphates.[28] After treatment at 1100°C for 7 h and

nitrogen incorporation up to 2·8 wt%, the single peak at 2·8056 ppm for original CDHA hydroxyapatite appears at 2·7484 ppm. The peak is very narrow and symmetrical and no second peak is found, indicating that there is no change in the PO_4^{3-} bonding state of apatite. Hence, no direct bonding between phosphorous and nitrogen is formed, like in the case of nitrided phosphate glasses and ceramics. The ^{31}P NMR spectra of Ceros 80 confirms the absence of P–N or P=N linkages in nitrogen containing apatite.[29] The single peak at 2·97 ppm for Ceros 80 hydroxyapatite containing 1·3 wt% of nitrogen, clearly indicates that phosphorous ions are forming linkages with only one kind of atoms, corresponding to the oxygen ion of the phosphate group. No second type of bonding can be detected.

It has been indicated[30] that thermal decomposition reaction of hydroxyapatite into α- and β-tricalciumphosphate is a reversible reaction and hydroxyaptite can be formed again by an annealing treatment. Only the formation of an amorphous β-tricalcium phosphate phase is an irreversible process but this phase is easily recognized in the NMR spectra. This fact explains the increase in the crystalline grade of hydroxyapatite by the thermal treatment in ammonia atmosphere.

The small changes produced in the lattice parameters of hydroxyapatite by nitrogen incorporation and the scarce modifications observed in XRD and ^{31}P NMR spectra suggest that hydroxyl groups, rather than phosphate groups, are substituted by nitrogen-containing ones. FTIR spectra are useful to consider the possibility of nitrogen incorporation by substitution of the hydroxyl ions of apatite. The FTIR-spectra of nitrogen containing CDHA (Fig. 8) and Ceros 80 apatites (Fig. 9) show four new bands at 3250, 2016, 1966 and 700 cm^{-1} which cannot be attributed to any calcium phosphate phase formed by phase transformation during heat treatments. These bands increase with nitrogen content and the relation between their intensities remains constant and must be attributed to only one nitrogen containing group. At the same time these bands increase, the OH bands of HA at 3570 and 630 cm^{-1} decrease and cannot be detected for nitrogen contents higher than 2·6 wt% [see Fig. 8(c)]. These results suggest that nitrogen-containing groups substitute the hydroxyl ions of HA during the ammonia treatments.

IR spectra of various nitrogen compounds groups have been compared to determine the entering groups. Amino and imino ions, $[NH_2]^-$, $[NH]^{2-}$, were the first considered groups, because of their similar size and structure to hydroxyl ions. However, their IR spectra hardly fit the data of this work[31] (Table 3). In particular, the sharp IR-band of nitrogen-containing apatite at 2016 cm^{-1} can not be explained by amino ions as incorporated substituents. The only good agreement found for the unassigned IR-bands of nitrogen-containing apatite were the IR-spectra of cyanamide $[CN_2]^{2-}$ compounds.[32] In Fig. 10, the infrared spectrum of $CaCN_2$ from Merck, Darmstadt (Germany) is compared to those of CDHA and Ceros 80 hydroxyapatites containing 3·7 and 2·1 wt% of nitrogen, respectively. The $[CN_2]^{2-}$-ion is linear and has only two IR active modi, which are the asymmetrical stretching modus ν_3, between 2130 and 1855 cm^{-1}, and the bending modus ν_2 at about 650 cm^{-1}. In cyanamide compounds like e.g. $CaCN_2$, bands between 3400 and 3200 cm^{-1}

Table 3. IR wavenumbers (cm^{-1}) of amino- and cyanamide ions compared to nitrogen containing apatite

Nitrogen containing apatite unassigned IR-bands	*NH_2^-/NH^{2-} (mode)*	*$CaCN_2$ (mode)*
3250	3500—3100 (ν_1,ν_3)	3341, 3240 (ν_1, ν_3 H–NCN)
2016	1650—1520 (ν_4)	2056 (ν_3)
1966	—	—
700	900—600 (ν_2)	669 (ν_2)

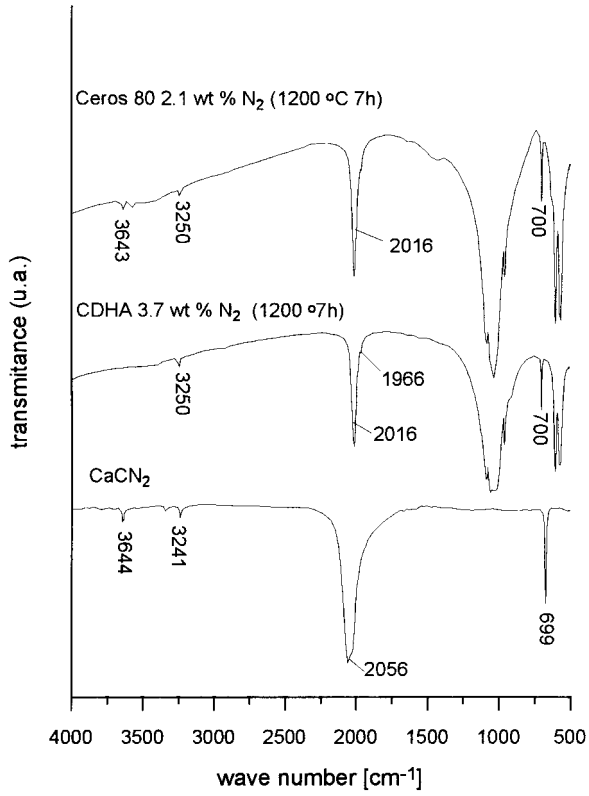

Fig. 10. IR absorption spectra of CDHA and Ceros 80 hydroxyapatites containing 3·7 and 2·1 wt% of N_2 respectively, compared to one of $CaCN_2$.

attributed to H–NCN bonds are normally observed. Table 3 shows that three of the four unassigned bands of the nitrogen-containing apatites could clearly be attributed to the vibration modes of $[CN_2]^{2-}$ and $[CN_2H]^-$-ions. It is suggested that the weak IR band at 3250 cm^{-1} corresponds to a stretching mode (ν_1 or ν_3) of $[H–NCN]^-$ ions. The intensive band at 2016 cm^{-1} could be attributed to the ν_3-mode and that at 700 cm^{-1} to the ν_2-mode of $[N–C-N]^{2-}$ ions. The attribution of the IR-band at 1966 cm^{-1} is not evident. Its wave number is characteristic of a stretching mode of $[CN_2]^{2-}$ groups, too. Its small deviation towards lower frequency and its low intensity provide the evidence for attribution to a ^{13}C-satellite of the ν_3-mode of $[CN_2]^{2-}$.

Taking into account the XRD and ^{31}P NMR data and the agreement between IR spectra of nitrogen-containing apatite and calciumcyanamide, it is suggested a mechanism of substitution of OH-ions by $[CN_2]^{2-}$ ions that could also explain the role of graphite in the nitridation process.

First, ammonia reacts with carbon to form cyanamide molecules (H_2CN_2):

$$2NH_3 + C \rightarrow H_2CN_2 + 2H_2 \quad (4)$$

Later, these molecules interchange with hydroxyl ions of apatite:

$$Ca_{10}(PO_4)_6(OH)_2 + H_2CN_2 \rightarrow Ca_{10}(PO_4)_6CN_2 + 2H_2O \quad (5)$$

Carbon analysis of nitrogen-containing samples confirm the proposed mechanism. As shown in Table 2, the carbon–nitrogen relation fits, within the error of the measurement and the inhomogenity of the samples, to the C/N-ratio in $[CN_2]^{2-}$ of 0·43. Also, the fact that no nitrogen was introduced in absence of graphite during ammonia treatment supports the model of formation of cyanamide ions, which are introduced into apatite structure substituting OH ions. A similar reaction is known for the synthesis of calciumcyanamide from calciumoxide.

$$CaO + 2NH_3 + 2C \rightarrow CaCN_2 + CO + 3H_2 \quad (6)$$

After ammonia treatments at temperatures above 1200°C a decrease in nitrogen content and a strong phase transformation are observed (Figs 2 and 3). XRD patterns (Figs 4 and 5) show that after treatments at $T = 1300$°C for 7 h and $T = 1200$°C for 16 h, apatite disappears, whereas $Ca(OH)_2$, CaO and graphite appear. This phase transformation is attributed to a reduction of phosphate to elemental phosphorus. From ammonia treatments of phosphate glasses and ceramics at similar temperatures, it is known that phosphate groups are reduced to elemental phosphorus or even to phosphine in the highly reducing atmosphere of carbon and ammonia.[17,18,29] In agreement with the observation of red phosphorus in the exit tube after high temperature treatments and the disappearance of phosphorous compounds in the XRD spectra, a strong reduction of phosphate tetraedra of apatite is suggested. The phosphate reduction destroys the apatite lattice. Thus, the sites of the $[CN_2]^{2-}$ groups disappear and the nitrogen content decreases. The chemical and physical properties of this new synthetic apatite will be further studied, taking into account possible applications as gas sensors.

5 Conclusions

Nitrogen has been incorporated into hydroxyapatite by dry ammonia treatments at temperatures between 900 and 1200°C in presence of graphite. Ammonia reacts with graphite during heat treatment forming CN_2^{2-}-ions. ^{31}P NMR, IR, and XRD data indicate that these cyanamide ions interchange with the moveable OH^- ions situated on the six-fold screw axis of apatite and cyanamidapatite, $Ca_{10}(PO_4)_6CN_2$, is synthesized.

Treatments at temperatures above 1200°C or long term treatments destroy the apatite lattice completely through phosphate reduction, the cyanamide ions loose their sites in the apatite lattice, and the nitrogen content decreases.

Acknowledgements

The authors wish to thank Dr. Isabel Sobrado and Prof. Jesús Sanz for the NMR experiments and the helpful discussion, as well as the CIDA Laboratory of CRISTALERIA ESPAÑOLA; S.A. for the C measurements.

References

1. Newman, W. F. and Newman, M. W., Nature of mineral phase of bone. *Chem. Rev.*, 1953, **53**, 1–138.
2. Takahashi, T. T., Tanase, S. and Yamamoto, O., Electrical conductivity of some hydroxyapatites. *Electrochem. Acta.*, 1978, **23**, 369–373.
3. Kay, M. I., Young, R. A. and Posner, A. S., Crystal structure of hydroxyapatite. *Nature*, 1964, **204**(12), 1050–1052.
4. Elliot, J. C., Mackie, P. E. and Young, R. A., Monoclinic hydroxyapatite. *Science*, 1973, **180**, 1055–1057.
5. Elliot, J. C., Bonel, G. and Trombe, J. C., Space group and lattice constants of $Ca_{10}(PO_4)_6CO_3$. *J. Appl. Cryst.*, 1980, **13**, 618–621.

6. Elliot, J. C., The problems of composition and structure of mineral components of the hard tissues. *Clin. Orth. Rel. Res*., 1973, **93**, 313–345.
7. Baravelli, S., Bigi, A., Ripamonti, A., Roveri, N. and Foresti, E., Thermal behavior of bone and synthetic hydroxyapatites submitted to magnesium interaction in aqueous medium. *J. Inorg. Biochem*., 1984, **20**, 1–12.
8. Young, R. A., Biological apatite versus hydroxyapatite at the atomic level. *Clin. Orth. Rel. Res*., 1975, **113**, 249–262.
9. Yamashita, K., Owada, H., Nakagwa, H., Umegaki, T. and Kanazawa, T., Trivalent-cation-substituted calcium oxyhydroxyapatite. *J. Am. Ceram. Soc*., 1986, **69**(8), 590–594.
10. Elliot, J. C. and Young, R. A., Conversion of single crystals of chlorapatite into single crystals of hydroxyapatite. *Nature*, 1967, **214**, 904–906.
11. Sudarsanan, K., Young, R. A. and Wilson, A. J. C., The structures of some cadmium 'apatites' $Cd_5(MO_4)_3X$. I. Determination of the structures of $Cd_5(VO_4)_3I$, $Cd_5(PO_4)_3Br$, $Cd_5(AsO_4)_3Br$ and $Cd_5(VO_4)_3Br$. *Acta Cryst*., 1977, **B33**, 3136–3154.
12. Wilson, A. J. C., Sudarsanan, K. and Young, R. A., The structures of some cadmium 'apatites' $Cd_5(MO_4)_3X$. II. The distributions of the halogen atoms in $Cd_5(VO_4)_3I$, $Cd_5(PO_4)_3Br$, $Cd_5(AsO_4)_3Br$, $Cd_5(VO_4)_3Br$ and $Cd_5(PO_4)_3Cl$. *Acta Cryst*., 1977, **B33**, 3142–3154.
13. LeGeros, R. Z., Trautz, O. R., LeGeros, J. P. and Klein, E. Carbonate substitution in the apatite structure (1). *Bull. Soc. Chim. France* 1968 1712–1718.
14. Binder, G. and Troll, G., Coupled anion substitution in natural carbon-bearing apatites. *Contrib. Mineral Petrol*., 1989, **101**, 394–401.
15. Mackie, P. E., Elliot, J. C. and Young, R. A., Monoclinic structure of synthetic $Ca_5(PO_4)_3Cl$, chlorapatite. *Acta. Cryst*., 1972, **B28**, 1840–1848.
16. Trombe, J. C. and Montel, G., Some features of the incorporation of oxygen in different oxidation states in apatitic lattice. I. On the existence of calcium and strontium oxyapatites. *J. Inorg. Nucl. Chem*., 1978, **40**, 15–21.
17. Pascual, L., Habelitz, S. and Durán, A., Nitridation of mixed alkali phosphate glasses. *Phys. Chem. Glasses*, 1996, **37**, 143–148.
18. Pascual, L. and Durán, A., Nitridation of glasses in the system R_2O–MO–P_2O_5. *Mater. Res. Bull*., 1996, **31**, 77–95.
19. Braun, M. and Hartman, P., ^{19}F and ^{31}P NMR spectroscopy of calcium phosphates. *J. Mater. Sci: Mater. Med*., 1995, **6**, 150–154.
20. Fowler, B. O., Infrared studies of apatites. I. Vibrational assignments for calcium, strontium, and barium hydroxyapatites utilizing isotopic substitution. *Inorg. Chem*., 1974, **13**, 194–207.
21. Rehman, I. and Bonfield, W., Characterization of hydroxyapatite and carbonated hydroxyapatite by photo acoustic FTIR spectroscopy. *J. Mater. Sci.: Mater. Med*., 1997, **8**, 1–4.
22. Steger, E. and Schmidt, W., Infrarotspektren von sulfaten und phosphaten. *Ber. Bunsenges*, 1964, **68**, 102–109.
23. Zhou, J., Zhang, X., Chen, J., Zeng, S. and de Groot, K., High temperature characteristics of synthetic hydroxyapatite. *J. Mater. Sci. Mater Med*., 1993, **4**, 83–85.
24. Fowler, B. O., Moreno, E. C. and Bown, W. E., Infra-red spectra of hydroxyapatite octacalcium phosphate and pyrolysed octacalcium phosphate. *Arch. Oral Biol*, 1966, **11**, 477–492.
25. Conley, R. T., *Espectroscopia Infraroja*. Ed. Alhambra S. A., Madrid, 1974.
26. Rodin, S. R. and Ducheyne, P., Plasma spraying induced changes of calcium phosphate ceramic characteristics and the effect on in vitro stability. *J. Mater. Sci. Mater. in Med*., 1992, **3**, 33–42.
27. Sudarsanan, K. and Young, R. A., Structural interactions of F, Cl and OH in apatites. *Acta. Cryst*., 1978, **B34**, 1401–1407.
28. Rotwell, W. P., Vaugh, J. S. and Yesinkowski, J. P., High-resolution variable temperature ^{31}P NMR of solid calcium phosphates. *J. Am. Chem. Soc*., 1980, **102**, 2637–2643.
29. Day, D. E., Structural role of nitrogen in phosphate glasses. *J. Non-Cryst. Solids*, 1989, **112**, 7–14.
30. Vogel, J., Hartmann, P., Alkemper, J., Günter, G. and Hfueß, H., ^{31}P MAS NMR and X-ray investigations of annealed hydroxy apatite. *Proceedings of the 5th Otto-Shott-Kolloquium*, Jena, Germany, 1994, p. 608.
31. Novak, A., Portier, J. and Bouclier, P., Étude par spectroscopie infrarouge des amidures de lithium, sodium et potassium. *C. R. Acad. Sci. Paris*, 1965, **t-261**, 455–457.
32. Fletcher, W. H. and Brown, F. B., Vibrational spectra and the inversion phenomenon in cyanamide and deuterated cyanamide. *J. Chem. Phys*., 1963, **39**(10), 2478–2484.